Thermal analysis on a novel natural convection flat plate collector with perforated tilted transparent insulation material parallel slats (TIM-PS) in Mediterranean climate

Marwa Ammar, Nahed Soussi, Ameni Mokni, Hatem Mhiri, Philippe Bournot

Energy Reports 10 (2023) 4064–4077

Contents lists available at ScienceDirect

Energy Reports

journal homepage: www.elsevier.com/locate/egyr

Thermal analysis on a novel natural convection flat plate collector with perforated tilted transparent insulation material parallel slats (TIM-PS) in Mediterranean climate

Marwa Ammar [a,*], Nahed Soussi [a], Ameni Mokni [a], Hatem Mhiri [a], Philippe Bournot [b]

[a] Laboratory of Thermal and Thermodynamic of Industrial Processes, National School of Engineers of Monastir, road of Ouardanine, 5000 Monastir, Tunisia
[b] Aix Marseille Univ, CNRS, IUSTI, Marseille, France

ARTICLE INFO

Keywords:
Flat plate air collector
Numerical simulation
TIM-PS
Natural convection
Volume flow rate
Thermal performance

ABSTRACT

The purpose of this research is the evaluation of heat transfer by natural convection in an innovative flat plate solar collector operating in natural convection mode. The design consists of inclined, perforated slats of transparent insulation material installed between the absorber and the glass cover. Hourly climatic data on the four specific days of solstices and equinoxes was used to investigate the behavior of the novel collector design in the city of Monastir; Tunisia. A comprehensive process, ANSYS FLUENT, was implemented to properly evaluate the thermal performance of the collector. In order to obtain accurate thermal properties of the smart collector façade unit containing the TIM-PS to exploit in the simulation, a validated three-dimensional finite volume model developed using the CFD software was used to solve the conductive, convective and radiative heat transfer properties of the system. We have explored in depth the effect of optical characteristics of the TIM-PS on the collector performance. Present research focuses on the analysis of thermal efficiency profile of flat plate collector with innovative façade in comparison with conventional collector for different climatic conditions. The analysis indicated that innovative façade collector's efficiency is highly influenced by solar intensity. It was found that TIM-PS façade can effectively reduce the convective heat losses through the front of collector. The simulation results show that perforated tilted TIM-PS offer better performance than conventional façade of collector during all the seasons of the year. Simulations performed for one year predict that with careful selection of the parallel slats properties, the new façade system can generate an efficiency up to 83% in June, 76% in September, 53% in March and 42% in December. The results of the thermal evaluation of this research will help guide the future development of this system, as we have demonstrated that the innovative façade collector can be used all year round. In conclusion, the TIM-PS have great potential and a very wide range of applications in the field of flat plate solar collector.

1. Introduction

The world is aware of the fact that global warming and the resulting climatic catastrophes are seriously compromising the survival of Humanity. As a result of an overwhelming necessity of immense energy for modern society, it is extremely valuable and desired to increase the availability of renewable and sustainable sources of energy conversion. The development and exploitation of renewable energy technologies is creating significant variations in the global power mix. Within this trend, solar energy has major opportunities for novel solutions. Solar thermal energy has been well explored and used in past decades as one of the green energy sources.

A variety of solar energy collection devices and systems have been applied in many areas, due to the huge demand for energy in the residential and agriculture fields. The space heat fulfilled a physiological requirement of comfort of the humans. In the industrial field, it allows the transformation of materials and the heating of industrial processes. In the building, a heating equipment ensures the thermal comfort of users. Of the many types of solar collectors, the flat plate collector (FPC) and the evacuated tube collector (ETC) are the most common in residential and building heating. Indirect flat plate solar collector dryers are a common technology in solar drying. The Flat Plate collector performs the worst among all the available solar panels, but nevertheless it is still widely chosen thanks to its affordability and simplicity of service (Kim et al., 2019). The first operation using this type of collector was the

* Corresponding author.
E-mail address: ammarmriwa@gmail.com (M. Ammar).

https://doi.org/10.1016/j.egyr.2023.10.052
Received 4 May 2023; Received in revised form 22 September 2023; Accepted 16 October 2023
Available online 31 October 2023

Nomenclature

A_c	L*W, Gross collector area [m^2]
C_p	specific heat of air [J/kg K]
e	height of the air gap [m]
e"	slat's height [m]
e"/e	relative height of slats
h	heat transfer coefficient [W/m^2 K]
h_W	convective heat transfer coefficient [W/m^2 K]
h_r	radiative heat transfer coefficient [W/m^2 K]
I	global irradiance incident on solar air heater collector [W/m^2]
$\dot{m}$	mass flow rate of air [kg/s]
T_a, T_{amb}	ambient temperature [K]
T_{abs}	absorber temperature [K]
T_f	average fluid (air) temperature [K]
T_{fi}	inlet fluid temperature [K]
T_{fo}	outlet fluid temperature [K]
T_g	glass temperature [K]
T_{pm}	average temperature of heated plate (absorber) [K]
T_{sky}	sky temperature [K]
U	air velocity inside the air duct [m/s]
U_b	bottom heat loss coefficient [W/m^2K]
U_e	edge heat loss coefficient [W/m^2K]
U_L	global heat loss coefficient [W/m^2K]
U_t	top heat loss coefficient [W/m^2K]
V_f	mean fluid velocity [m/s]
W	collector's width [m]
W_v	wind velocity [m/s].
Q_u	useful energy gain [W]
$\dot{v}$	air volume flow rate [m^3/s]

Greek symbol

α	absorber plate absorption coefficient
β	coefficient of expansion at constant pressure
ε	emissivity of absorber plate
ρ_f	air density [kg/m^3]
ρ_0	air density at the reference temperature [kg/m^3]
σ	Stefan-Boltzmann constant = 5.6710^{-8} [W/m^2. K^4]
τ	transparent cover transmittance

Abbreviations

CFD	Computational Fluid Dynamics
FPC	Flat Plate Collector FPSAC, Flat Plate Solar Air Collector
ITSD	Indirect Type Solar Dryers
PMMA	Poly-Methyl-Methacrylate
TIM	Transparent Insulation Material
TIM-PS	Transparent Insulation Material Parallel Slat

agricultural drying of vegetables and fruit. This technique is the oldest agricultural food preservation treatment undertaken by farmers in the world. Because it requires no additional energy, this process is always preferable to other methods. However, traditional air-drying also has its drawbacks (Saini et al., 2017). In return the indirect type solar dryers (ITSD) can offer a better solution for the processing of agricultural products. The FPSAC is the main component of the ITSD. It captures the sun's rays and transforms them into a heat source capable of heating the air passing beneath the absorber. This hot air is pushed towards the processing area where the food will be dried.

Work on air heating systems using forced convection with fans or pumps is increasing worldwide. However, the principle of energy recovery using natural convection systems is still little exploited, probably because of the mediocre thermal efficiency compared with the performance of forced airflow systems. However, this factor should not prevent the use of this type of system. In the final analysis, natural convection recuperates are the most widely used in various fields, particularly in the agricultural drying industry. In the context of an air collector functioning in natural convection mode, the thermal losses act on the air volume flow rate circulating below the absorber. The rise of the losses reduces the air volume flow rate inducing a reduction of the efficiency. In the study by Rani and Tripathy (2020), the effect of solar intensity and air mass flow rate on air temperature, thermal efficiency, heat transfer coefficients and heat loss coefficients are discussed. This research focuses on the analysis of the temperature profile, heat transfer characteristics and thermal efficiency of a flat plate solar air collector (FPSAC) at different air mass flow rates. The analysis indicated that the useful heat gain, air heat transfer coefficient, and thermal efficiency of the collector were not very strongly influenced by solar intensity. It was proved that air with a mass flow rate of 0.01, 0.015 and 0.02 kg/s respectively achieved a greater convective heat transfer coefficient of 30.73%, 57.88% and 96.40% respectively as compared to that of 0.006 kg/s. By raising the air mass flow rate from 0.006 to 0.02 kg/s, thermal efficiency rises dramatically from 22.53% to 32.3%, demonstrating that the flat plate solar air collector operates optimally at a higher air mass flow rate, i.e. 0.02 kg/s.

Inside the space of air confined between the absorber and the glazed cover, a movement of natural convection takes place because of the buoyancy force of Archimedes and the difference in temperature which exists between the two plates. This convective movement within the cavity generates thermal losses to the outside through the glazed cover supposed to be the cold plate of the cavity, these losses represent approximately 95% of the losses of the collector. The thermal performance of the collector is strongly linked to the intensity of these losses. This intensity of the losses is in turn dependent on the shape and the angle of inclination of the cavity with respect to the horizontal (Duffie et al., 1985). A flat plate solar collector for residential applications has a number of heat loss coefficients, ranging from 5.5 W/m^2 K for the most selective surfaces to 10–11 W/m^2K for black absorbing surfaces (Groenhout et al., 2002).

(Eismann, 2015)studied the empirical correlations that have been established concerning the phenomenon of natural convection in the air gap of a flat air collector. The most widely used equation is that of (Hollands, 1965), which dates back forty years. K. Hollands (Hollands, 1965) showed that for a Rayleigh number less than the critical number $Ra_c = 1708$, the fluid layers are stagnant and the Nusselt number is equal to unity$Nu = 1$. When the flow Rayleigh number reaches the critical number, the fluid flow takes a new form from stagnant to a regular roll form. The natural convection flow is very sensitive to the angle of inclination of the enclosure and the temperature difference between the two walls.

(Varol and Oztop, 2008) have suggested an innovative method of corrugated absorber within a tilted collector. The solution was realized by assuming isothermal boundary conditions of absorbers and collector covers. The governing parameters are taken as Rayleigh number (from 1×10^6–5×10^7), tilt angle (from 20° to 60°), wavelength (from 1.33 to 4) and aspect ratio (from 0 to 4). This survey showed that the shape of the enclosure affects the heat flow and thermal fields, which are considerably modified. The heat transfer achieved by corrugated enclosures is greater than that by flat surfaces.

The optical power of solar transmission is the main property required of solar collectors, and more specifically the transmission of solar energy.

Because of the combination of excellent thermal insulation properties with powerful radiation transmission capabilities in the solar spectrum, transparent insulation materials (TIM) are a type of material with

very interesting characteristics in terms of thermal conversion of solar radiation.

Transparent insulating materials (TIMs) are considered to be one of the most promising technologies for thermal insulation and solar energy transmission. Transparent insulating materials have low thermal conductivity and high transmittance in the visible bands.

The production of TIMs has not been simple and cost-effective in the past, but with technological advances it has become possible to produce TIMs systems with thermal transmittance (U-values) of less than 1 W/m^2. K and solar transmittance of more than 50% (Paneri et al., 2019). Transparent insulating material (TIM) is characterized by its ability to efficiently recover and conserve solar thermal energy, minimizing heat loss. It enhances insulation capacity by slowing the flow of thermal energy within small air gaps or spaces evacuated in materials with low thermal conductivity. The ability of TIMs to reduce heat loss and ensure solar transmission varies according to operating temperature, geometric structure and type of material. So, to characterize TIMs for different applications, the thermal transmittance (U-value) and the solar transmittance are two essential parameters.

Transparent insulation materials (TIMs) have a remarkable solar thermal energy recovery effect, and are being used progressively and massively in energy-efficient buildings. What sets TIMs apart is their flexibility, light weight and great applicability.

The outstanding qualities of TIMs suggest a wide range of new applications for economical solar heat recovery through high temperature flat plate collectors, integrated storage systems for storage, building façade and roof heating, and solar desalination, in addition to outdoor applications (Gorgolis and Karamanis, 2016; Schaefer and Lowrey, 1992; Rosenfeld et al., 2001). The materials and structures of TIMs have been investigated both theoretically and experimentally (Jia et al., 2018). TIMs have achieved a parallel light transmission of more than 70% for hexagonal honeycomb (Hollands et al., 1992; Plaizer, 1992) TIMs have also shown significant thermal insulating power due to the limitation of thermal convection (Fuji et al., 2015).

Synthetics such as polyethylene (TPX), poly-methyl-methacrylate (PMMA), polytetrafluoroethylene (HFL), polyester carbonate (TPX), polytetrafluoroethylene (HFL), polyester carbonate (APEC), polyether sulfone (PES), FEP-Teflon (FEPT) and polycarbonate (PC). (PC), are widely chosen for TIM glazing applications (Ming et al., 2022). A reason for the adoption of such materials is because of their poor thermal conductivity (<0.5 W/mK) versus that of glass (~1 W/m·K). In these materials, their relatively good visible transmittance also renders them adequate to be embedded in glazing.

To ensure increased energy efficiency and excellent indoor environmental quality, a smart glazing device, a transparent insulating material integrated with the window, is being studied in the investigation of (Sun et al., 2021). This smart window system aims to provide increased thermal resistance as well as dynamic control of solar energy and daylight admission and thus contribute to the international aspirations of reducing building-related CO_2 emissions.by integrating a transparent insulation material (TIM). This system automatically regulates the admission of solar heat and natural light into the building by adapting to a changing environment and taking advantage of the increased thermal resistance and diffused daylight by the TIM integrated into the window. To demonstrate the application of this window system in buildings and provide guidance for future stages of design and material development, building simulations of a typical office with (TT PS-TIM) installed in the climates of London, Stockholm, Rome and Singapore. TT PS-TIM systems with different material properties were thermally characterized and optically characterized. This research report provided an overview of the evaluation of the new window unit design concepts using severe numerical methods of modeling. The yearly results of the simulation predict that, with thorough preparation of the material properties of the thermotropic material, the adoption of the TT PS-TIM window arrangement yields up to 27.1% energy saving than a conventional double glazed window arrangement in the climate modeled in Rome.

In the study of (Sun et al., 2017) an improved window system concept, involving the interleaving of parallel transparent/translucent plastic slats between glass panes to form a transparent parallel slat insulating material (PS-TIM), is considered as a technology for improving the thermal resistance performance of window systems, while at the same time allowing for higher illumination levels. This investigation has been conducted to determine the optical performance of a double-glazed window containing PS-TIM systems with different slat pitches, slat tilt angles, as well as transparent and translucent slat materials by studying the ray tracing method. The main impacts of this operation on daylighting performance are as follows: PS-TIM with translucent slats provide better daylighting conditions than conventional double glazing: they are likely to contribute to an increase in the annual working day rate in daylight, with illuminance in the useful range up to 79%. They promote a balanced distribution of daylight in the room and limit the risk of reflection. If PS-TIM is used in a high latitude location, smaller slats pitches are required to ensure maximum useful daylighting.

The work, carried out by Garcia et al. (2019), explores the inclusion of convective barriers between the absorption plate and the glass cover to increase the thermal efficiency of the solar collector. By use of such barriers, the cavity between the absorber plate and the glass cover is limited, which can reduce the heat loss under certain conditions. The experiment conducted using four solar collectors with one to four convective barriers. The findings proved that there is no significant variation in the absorption of solar radiation since the maximum thermal efficiency remains unchanged. Nevertheless, the incorporation of barriers involves significant variation on heat loss. The experiment records indicate such changes in heat loss as − 2.2%, − 5.3% and 2.9% for two, three and four barriers, respectively.

Hence, the following survey explores feasible enhancements of thermal efficiency of the existing flat plate solar collectors currently installed in domestic air heating systems and in agricultural product drying systems. The design and specification of the glazed envelope, which is responsible for a significant portion of the total heat loss in solar air collectors, is a key factor in determining the overall energy consumption. To address this problem, an innovative transparent façade system consisting of parallel slats of transparent insulating material sandwiched between the glass cover and the absorber plate to form a parallel slat transparent insulation material system (TIM-PS) is proposed as a potential solution. This paper provides an overview of the development of a new transparent multi-effect intelligent flat plate solar collector cover, which provides energy performance optimization and reduction of convective losses to the exterior environment by integrating a transparent insulation material (TIM). The analysis of the performance of the innovative solar air collector operating in natural convection mode containing slats made of transparent insulation material for different weather conditions has not received the necessary attention in the past. There are four times in year the season officially changes, and each change is marked by a specific point called the equinox or solstice. One term is used for the transition from winter to spring and from summer to autumn, and another for the transition from spring to summer and from autumn to winter; equinox and solstice days. The following overview of the performance of a flat plate air collector fitted with TIM-PS on typical days of the four specific days of solstices and equinoxes throughout the year is provided. In the simulation, a solar collector with a façade incorporating tilted and perforated TIM-PS is modeled, and the performance of the collector is calculated for each hour of the typical day for different weather seasons and climates.

The main objective of this study is to quantify the heat transfer by natural convection in the innovative and original system of the collector with TIM-PS, for the different climates of the whole year. The four seasons have been characterized by the four specific days, those of the spring and autumn equinoxes, and the winter and summer solstices dates. To achieve reliable thermal properties (thermal resistances) of the

innovative solar collector unit that incorporates the TIM-PS, a validated three-dimensional finite volume model, which was constructed with the aid of the CFD software ANSYS FLUENT 15.0, was selected to simulate the conductivity, convection and thermal resistance. The intention is to predict its effect on the thermal performance efficiency. Unsteady analysis is carried out to analyze the seasonal performance of the solar air collector during a whole day for the period from 6 am to 6 pm. A three-dimensional transient simulation of solar air collectors is considered in this work.

2. Methodology

2.1. Mathematical modeling of FPC

The equations for volume flow rates, mass flow rates, thermal efficiency parameters, heat losses, convective heat transfer and energy parameters are provided in depth in the following part of the paper.

Numerous assumptions are regarded in order to reach the nearest to the concrete case.

- The Flow is turbulent, three-dimensional and incompressible.
- Numerical transient modeling of a flat plate solar collector: The condition of unsteady state is applied for the analysis as the device is operating over a period from 6 am to 6 pm.
- The air is assimilated to an ideal and incompressible gas.
- The air enters the air duct (below the absorber) through the inlet and rises towards the outlet of the duct by the phenomenon of transfer by natural convection. Fluid motion occurs by natural convection.

  The air gap (confined between the absorber and the glass cover) undergoes a phenomenon of natural convection in a confined cavity.
- Thermo-physical properties are kept constant in all calculations with values calculated at the standard 25 ∘C temperature.
- Heat losses across the adiabatic walls are negligible.

Useful energy gained by air is given by the Hottel–Whillier Bliss equation which was reported by Duffie and Beckman (1980)(Duffie et al., 1985);

$$Q_u = \dot{m}\mathrm{Cp}(T_{fo} - T_{fi}) = hA_c(T_{pm} - T_f) \tag{1}$$

where $\dot{m}$ is the mass flow rate of air (kg/s), Cp is the specific heat,T_{fo} is the outlet fluid temperature,T_{fi} is the inlet fluid temperature, h is the convective heat transfer coefficient, T_{pm} the average temperature of the absorber plate, T_f the average air temperature.

$$\dot{m} = \rho \quad \dot{\vartheta} \tag{2}$$

$\dot{\vartheta}$ is the volume flow rate, ρ is the fluid density.

The collector's thermal performance is then achieved through the principle of the ratio below; the quotient between the useful energy by the overall solar energy power captured by the collector. It is determined through the following formula commonly used;

$$\eta = \frac{Q_u}{A_c \times I} \tag{3}$$

Thermal dissipation occurring from the solar collector to the surrounding area manifested as three types of processes (Tuncer et al., 2020);.

$$\mathrm{U_L}=\mathrm{U_t}+\mathrm{U_e}+\mathrm{U_b} \tag{4}$$

U_t,U_e, $U_b$represent the respective top, edge and bottom heat coefficients. Upper heat transfer factor of the collector is explained by the following formula:

$$U_t = h_W + h_r \tag{5}$$

$h_W$represents the convection heat transfer factor from glazing towards the surrounding area, calculated as in the equation below;

$$h_W = 5.7 + 3.8W_v \tag{6}$$

$W_v$represents the wind speed.

$h_r$means the radiant heat transfer factor from glass cover to the surroundings, stated as below;

$$h_r = \sigma\varepsilon\left(T_{sky} + T_g\right)\left(T_{sky}^2 + T_g^2\right)\frac{(T_g - T_{sky})}{(T_g - T_{amb})} \tag{7}$$

2.2. Numerical modeling

A numerical analysis is carried out with the help of ANSYS FLUENT software to develop a numerical model, based on the experimental configuration of the study of (Bahria et al., 2013). In the current survey, a 3D model of a flat collector is established; at first, a simple conventional FPC is constructed. Validation studies are carried out to evaluate the realistic performance and check the design of the simulation model of a conventional FPC. Then, a flat plate collector with parallel slats of transparent insulation material is modeled. Boundary conditions for limits are set before the investigation of the mesh independency. After the verification of numerical model and boundary conditions, different parameters are studied on the FPC performance and volume flow rate.

In order to numerically investigate the fluid flow distribution as also as the heat transfer inside the various components of the collector, the fluid flow is considered to be three-dimensional, unsteady state, incompressible and viscous flow.

The flow is modelled by the Navier-Stocks equations. ANSYS FLUENT solves conservation equations for mass and momentum and equation for energy conservation. Based on the above assumptions the flow inside the collector governed by the continuity, momentum and energy as follows;

- Continuity Equation:

$$\frac{\partial\rho}{\partial t} + \nabla.(\rho\vec{v}) = 0 \tag{8}$$

- Momentum Equation:

$$\frac{\partial(\rho\vec{v})}{\partial t} + \nabla.(\rho\vec{v}\vec{v}) = \nabla p + \nabla.\left[\mu\left(\nabla.\vec{v} + \nabla\vec{v}^T\right)\right] + \rho\vec{g} + \vec{F} \tag{9}$$

- Energy equation:

$$\frac{\partial(\rho E)}{\partial t} + \nabla.(\vec{v}(\rho E + p)) = \nabla\left(k_{eff}\nabla T\right) + S_h \tag{10}$$

$S_h$is the radiation source term.

The air density variation follows the Boussinesq approximation ~~in ANSYS FLUENT~~, according to the Boussinesq approximation;

$$(\rho_F - \rho_0) = -\rho_0\beta(T - T_0) \tag{11}$$

β is the thermal expansion coefficient of air, it is dependent to temperatureT_0.

2.2.1. Solution techniques

For the solution of the above equations, while taking into account the boundary conditions and assumptions, the procedure chosen is based on the finite volume method. The three-dimensional solver 'Double-Precision' has been chosen for the resolution of the equations, thus a 'Serial' processing option has been adopted. The 'Pressure-Based' segregation solver was chosen and applied. The governing equations are solved sequentially, separated from each other, and linearized implicitly with respect to the dependent variable of the equation. The governing

differential equations have been solved numerically using the finite-difference method, and the transient problem was formulated using an implicit scheme that yields a stable solution for any grid size and time.

As there is no generalized turbulence model that covers all ranges of flow, laminar or turbulent. The process of choosing a turbulence model is not only dictated by the type of flow, but also by the availability of computing power and the desired accuracy. For the case of our flow model, the buoyancy driven air flow in the air gap and the heat transfer fluid flow in the air channel are the operative elements in identifying the suitable turbulence model; the standard k-ε turbulent model was employed to describe the buoyancy driven flow inside the air cavity. It is worth mentioning that the boundary layers of natural convection are not restricted to laminar flow, as is the case for forced convection, hydrodynamic instabilities can be encountered. Rayleigh-Benard convection which takes place inside confined air gap between absorber and transparent cover; is characterized by large cellular motion (Altaç and Uğurlubilek, 2016; Choi and Kim, 2012). The standard k-ε model was chosen as the computational procedure to close the mean flow equation system. It is in fact, a semi-empirical model based on the Boussinesq concept that relates Reynolds stresses to the mean strain rate.

ANSYS FLUENT features five radiation models. However, only the following two models are particularly suited to the simulation of radiation inside a confined cavity: the S2S (Surface to Surface) model and the DO (Discrete Ordinates) model.

The surface-to-surface radiation model can be used to account for radiation exchange within an enclosure of gray-diffuse surfaces. The fundamental assumption of the S2S model is to disregard any absorption, emission or scattering of radiation; consequently, only "surface-to-surface" radiation should be considered for analysis.

The S2S model is not suitable in the presence of obstacles within the volume to be analyzed.

In addition, the creation of form factors requires extremely high RAM memory capacities, increasing progressively as the number of surfaces increases.

It is therefore recommended to select the DO (Discrete Ordinates) model for solving radiative heat transfer. From among the various five radiation models available in Fluent, the 'DO' (Discrete Ordinates) model is the most efficient for solving heat transfer problems.

It is widely used, since it is the most efficient model for solving radiation problems with semi-transparent walls and participating and non-participating media, as well as being reliable and computationally short.

For the momentum and energy equations; a first order Upwind scheme is adopted. The SIMPLE algorithm, a semi-implicit method for the pressure related equations, is adopted for the continuity equations.

2.3. Physical domain, boundary conditions

The first designed air collector model is based on Bahria's experimental geometry (Bahria et al., 2013). Experimental model, serving for the numerical model verification and validation. Once the model is validated, the same model will be regarded under the same dimensions of the collector and the same boundary conditions, including the inclined perforated TIM-PS.

The solar air collector, designed with length of 1.93 m and width of 0.93 m having an air duct of height 0.04 m and air gap of height 0.02 m, below the air duct there is an insulation layer of height 0.04 m, is illustrated in Fig. 1 The collector operates in natural convection mode; it is then tilted with respect to the horizontal plane with an angle of 35°. It contains a single 0.004 m transparent glass cover with a solar transmissivity and absorptivity of 84% and 6% respectively. The manifold is equipped with a selective absorber ($\varepsilon = 0.1, \alpha = 0.9$). The air enters the air duct under the absorber plate through the lower inlet and follows the flow path before exiting through the upper outlet. The bottom support of the collector uses a 0.04 m thick polystyrene sheet for efficient heat thermal insulation.

The second model of the innovative vertical collector has the same dimensions and contains seven parallel slats of transparent insulation material, (Fig. 2) this innovative solution is proposed in order to reduce the heat losses through the front of the collector. The slats are made with transparent polymathic methacrylate (PMMA) with a transmissivity of$\tau = 0.92$. The TIM-PS are perforated and have the same width as the air gap of 0.935 m. The transparent slats are placed in a location that does not affect the absorber. The slats are inclined at an angle of + 45° to the vertical plane of the transparent cover. The seven slats subdivided the air gap from one cavity into eight sub-cavities, spaced at 0.241 m intervals between slats.

When conducting a numerical analysis, the term that expresses the numerical intervals is referred to as the boundary condition. Boundary conditions should be set correctly in order to obtain accurate and realistic results. The equations have been solved by imposing specific boundary conditions that approximate the real case of the collector's functioning and environmental conditions.

The inlet pressure condition is set as follows; at the inlet of the duct with a constant ambient temperature $T_{in} = T_{amb}$. At the outlet of the air

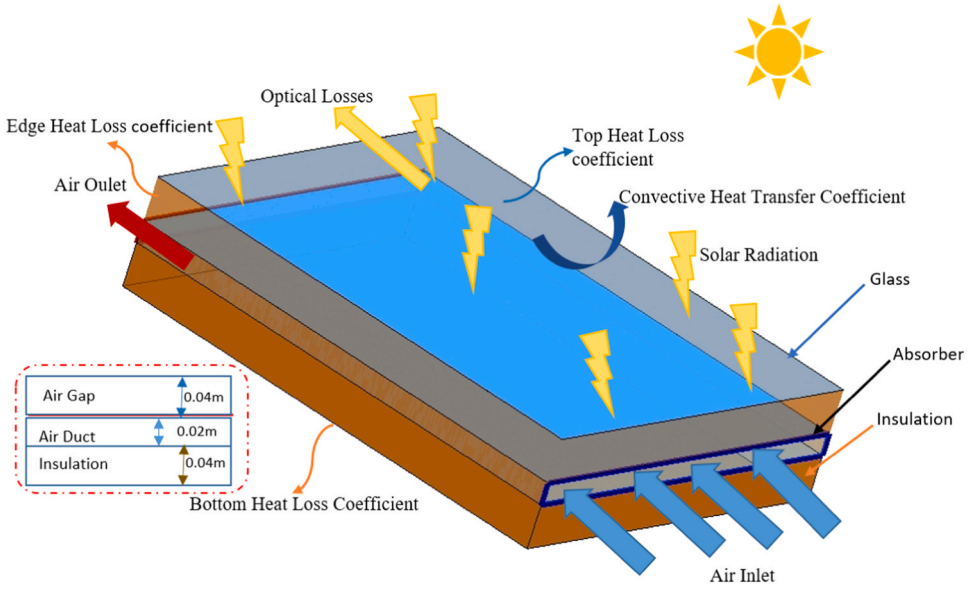

Fig. 1. Structure of The Simple FPC with Thermal and Optical Loss Balance.

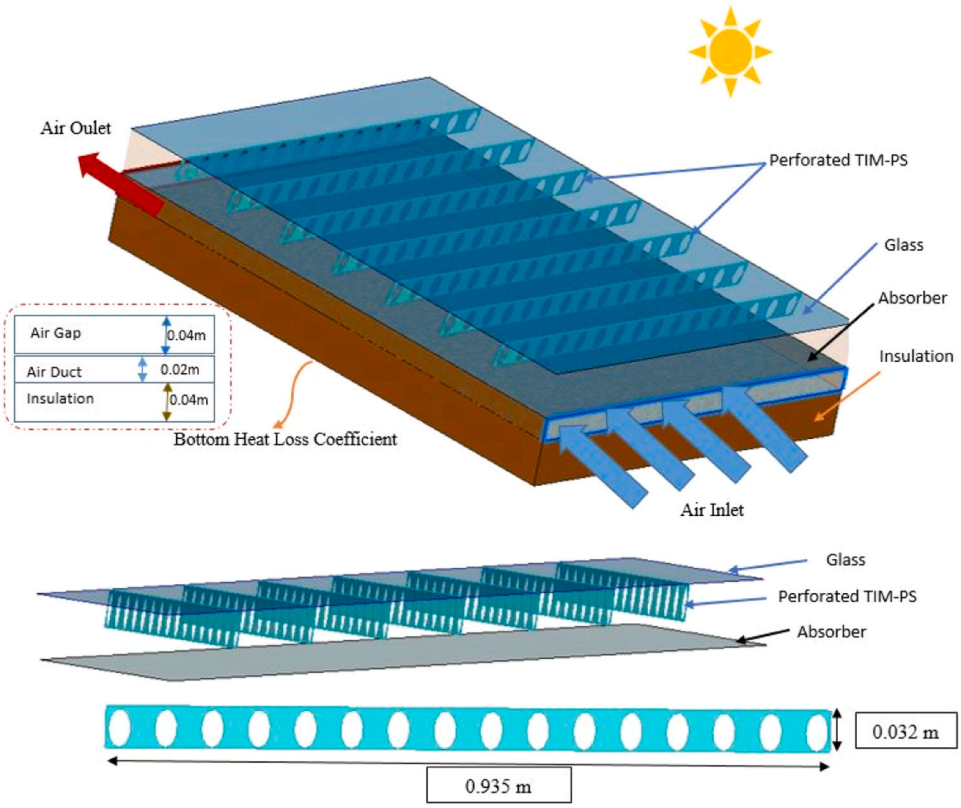

Fig. 2. Structure of novel FPC with perforated TIM-PS with Zoomed View for The Perforated TIM Slat.

duct a pressure outlet condition is applied, where the static pressure is set to the ambient pressure. An adiabatic wall with zero heat flow is considered at the side walls and below the collector, they are provided as "adiabatic wall". For the transparent cover of the collector, a semi-transparent wall is used with a "mixed" condition, which specifies the occurrence of radiative as well as convective exchanges at the transparent cover with 84% transmissivity. The absorber wall is considered as a selective wall with 10% emissivity and 90% absorptivity.

The Boussinesq approximation (Eq.11) is used to model the flux due to buoyancy.

The first case is considered as the base case which has the same geometry properties as (Bahria et al., 2013).

The simulations of the collector performance were performed in one-hour time steps for a whole day considering the meteorological data for Monastir city. Depicting various weather conditions including temperature and solar radiation intensity over four specific typical days in a year which were chosen to show the different ways in which TIM-PS glazing systems influence the performance of the collector.

The ambient condition simulation was conducted with the mean values at 1-hour interval for a full day of investigation. The variables of the effect of the air outlet temperature and the absorber temperatures are to be determined and discussed.

2.4. Mesh generation

The " grid " is the fundamental sequence in a CFD simulation. The meshing is the subdivision into a specific amount of sub-domains. An adequate mesh model has a significant effect on the convergence, the reliability of the resolution and the time saving of the calculations.

The most suitable mesh configuration for solar air collector was evaluated based on unequal mesh sizes (elements). The computational model involves a hexahedral mesh (Fig. 3).

Table 1 shows the various mesh parameters tested for solar air collector. By using different mesh sizes and examining the numerical air velocity profiles obtained in the central region of the collector air duct. An appropriate balance must be found regarding the computational performance and the choice of the number of cells.

Fig. 4 depicts the variation in sensitivity of the air velocity profiles at the middle region of the channel for the four distinct mesh sizes. Simulations results with meshes 3 and 4 give the same air velocity profiles, thus from node number 671,470, the results become independent of node's number. In an effort to balance computational relevance with the time required for convergence, mesh 3 was retained for the entire analysis. The use of wall functions is essential to match the wall background. The resolution of the boundary layer contributes considerably to the reliability of the calculations of the wall shear stress and the heat transfer coefficient, it is important that the boundary layer is covered by an appropriate mesh. It is critical that the boundary layer is covered by a sufficient number of cells to achieve a certain $y+$ criterion. The convergence criteria chosen are 10^{-6} for the energy equation and 10^{-3} for each of the velocity, continuity, turbulent propagation and turbulence kinetic energy equations.

3. Results and discussion

We propose to examine the performance of the new designed collector including tilted perforated TIM-PS for four specific days of solstices and equinoxes in an outdoor environment during the months of December, March, June and September for a Mediterranean climate. The investigation will focus on the climate of Monastir, Tunisia. In order to facilitate the examination of a large amount of results we are using the CFD software. As an investigation, the influence of tilted perforated slats fitted to the inside wall of the transparent cover under several weather scenarios, on the performance of the air collector are evaluated. CFD simulations for different cases were performed with different values of ambient temperature and radiation. The simulations of the FPC efficiency were performed in one-hour time steps for whole days considering the meteorological data for Monastir city.

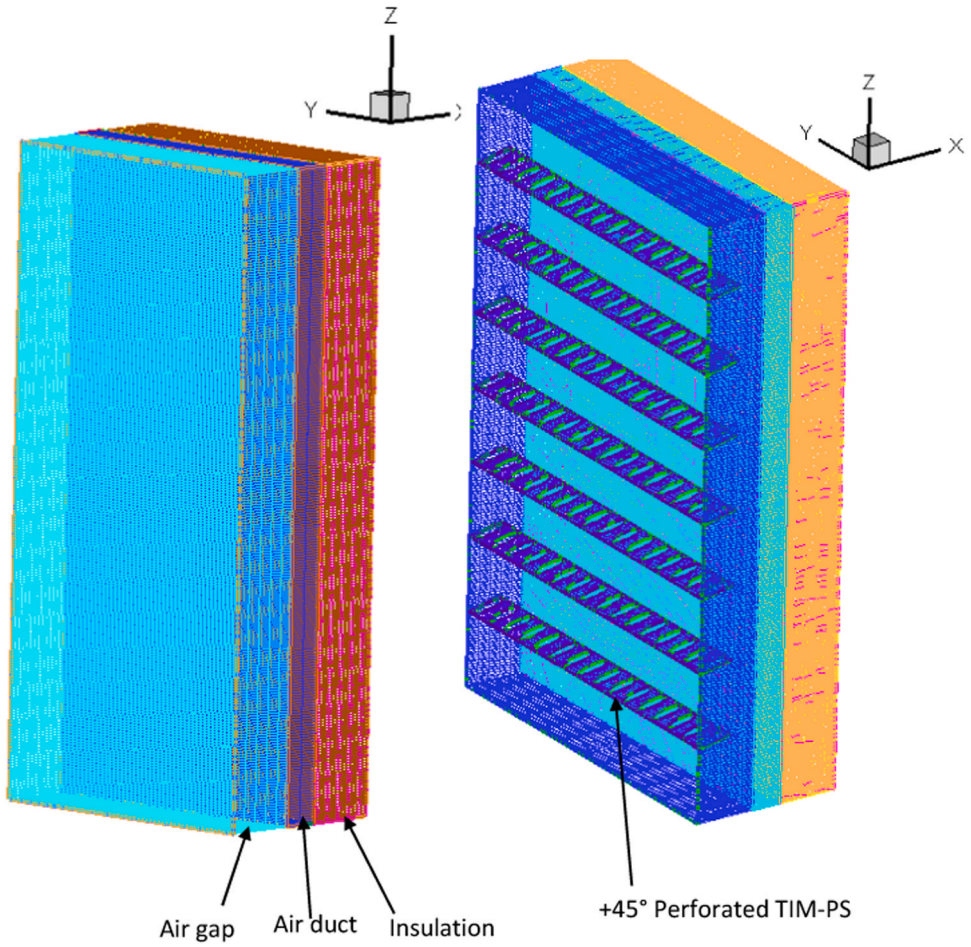

Fig. 3. Mesh Distribution of The Grid System.

Table 1
Number of Cells, Faces, And Nodes of the Four Mesh Design.

	Mesh 1	Mesh 2	Mesh 3	Mesh 4
Cell	366561	417625	554760	641520
Face	1188928	1354216	1781382	2059479
Node	455464	518600	671470	776016

3.1. Model validation

Validation of the model is carried out using both data available in the literature and results calculated using commercial software. The thermal efficiency values derived from the current three-dimensional numerical simulations are compared with the experimental values reported previously by the authors of the study by (Bahria and Amirat, 2013). The collector's geometry is described in Section 2.2. The validation case is based on a 35° inclined collector.

The assumptions taken into account are as follows;.

- The flow is considered to be turbulent; the standard k-ε turbulent model was employed.
- The unsteady flow mode has been adapted to the collector simulation for a daily time period between 7.45 am and 5.45 pm.
- In the full simulation, and also for the purpose of validating the model, the radiative heat transfer was solved using the discrete ordinate (DO) radiation model. The evolution of the daily radiation (illustrated in Fig. 5) and the ambient temperature are input in FLUENT.

The instantaneous thermal performance plots derived from numerical simulations and that found through experimental methods are presented in Fig. 6.

On the basis of the results achieved from the numerical simulations, we note a satisfactory accordance between the current numerical results and the experimental data of (Bahria et al., 2013), with an admissible deviation that does not reach 4.7%. The minimum value of the deviation in percentage is 0.28%, so on the basis of the excellent agreement among the numerical and experimental results, we may conclude the adequacy of our numerical model.

3.2. FPC with titled perforated TIM-PS

All numeric analyses were realized with a 3D model. Both a conventional and a novel collector including perforated tilted TIM-PS model (Fig. 7) were numerically analyzed. Through numerical evaluation, the outlet temperature of the FPC, the air volume flow rate and the thermal efficiency have already taken part in this study under various environmental conditions. For the purpose of the analysis, the reading of the results as well as the contour of the numeric FPC models has been performed.

Thermal properties of solid and fluid materials used in the numerical analysis are provided within Table 2. Regarding the thermophysical properties of the air were selected by constant. On the basis of the findings of earlier studies (Ammar et al., (n.d.)) and (Ammar et al., 2022), the required geometrical and material parameters of the TIM-PS were established. A suitable ratio e" (height of the lamellae) / e (height of the air gap) = 0.8 was achieved. As a result, following this ratio, the height of the TIM-PS should be set at 0.032 m in the case of the collector,

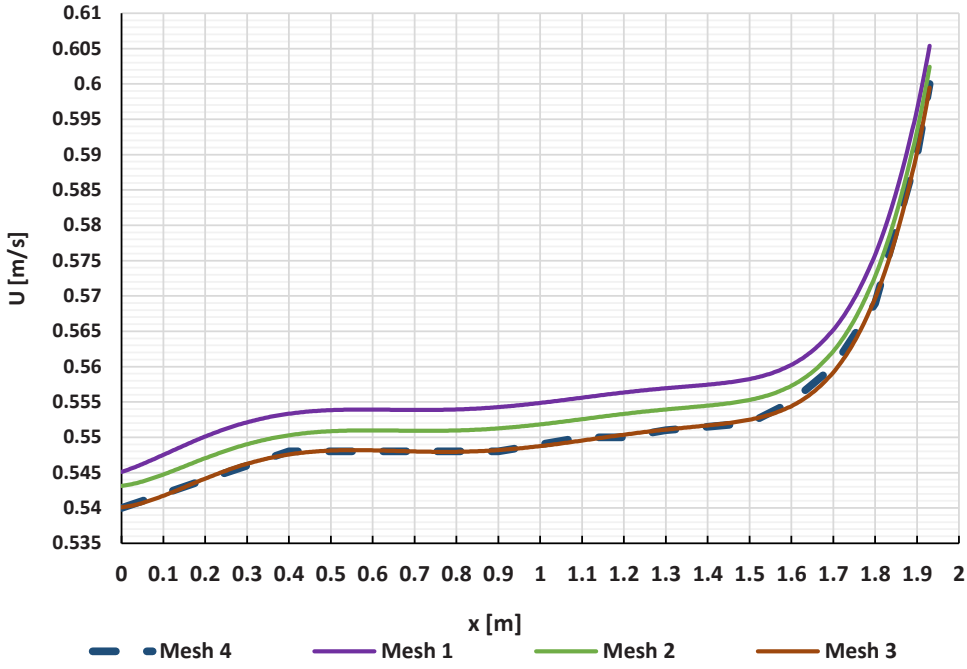

Fig. 4. Sensitivity of Results To the Mesh.

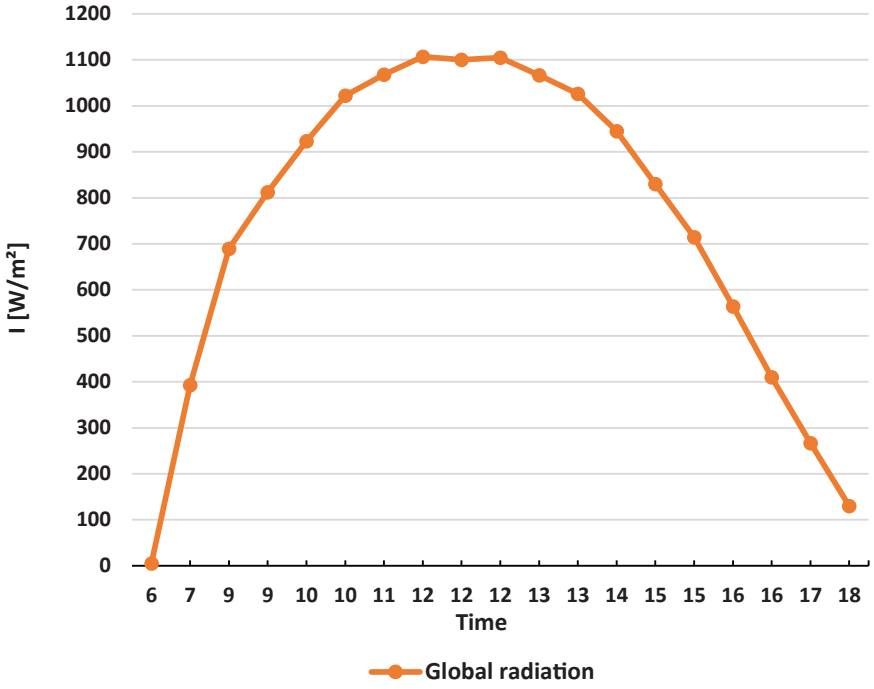

Fig. 5. Global Solar Radiation as A Function of Time for Experimental Data.

with an air gap height of 0.04 m. (see Table 3). The values of latitude, longitude and irradiance in the region of Monastir are reported in Table 4.

3.2.1. *Thermal efficiency*

Simulations were performed for four different typical days representing the four specific days of solstices and equinoxes in an outdoor environment during the months of December, March, June and September on the simple conventional solar collector system (Fig. 1) and the one with perforated and tilted slats of transparent insulation material (Fig. 2) on location in Monastir.

Monastir's climate was a subtropical steppe climate; in Monastir, summers were short, hot, humid, dry and clear, and winters were long, cool, windy and generally clear. Fig. 8 illustrates the fluctuations of average temperature and sunshine hours over the year in the city of Monastir. Over the year, the average temperature varies from 285.14 K to 301.14 K. In Monastir, the months with the greatest number of hours of daily sunshine are June and July, with eleven hours per day. In total, there are 395.49 h of sunshine during June. The months with the lowest number of hours of sunshine per day in Monastir are January, November

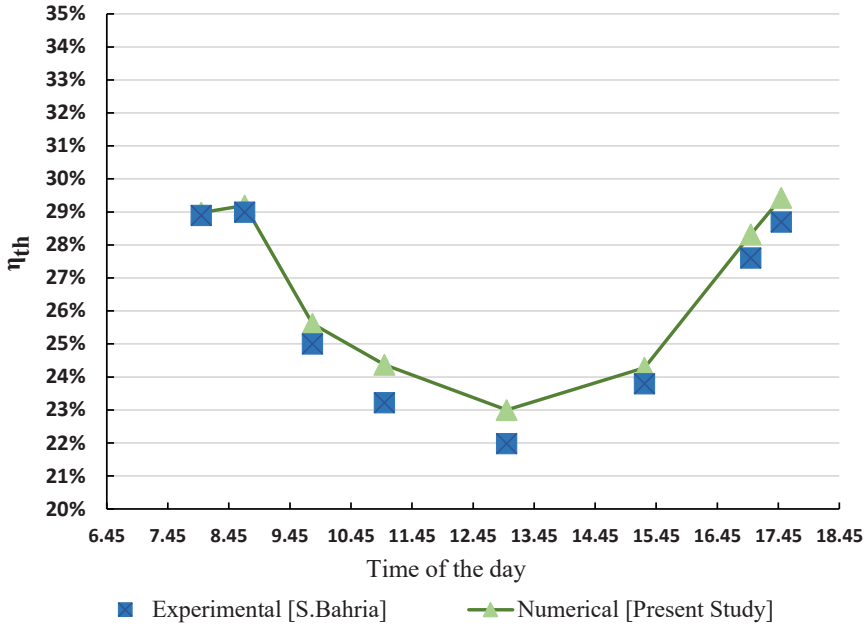

Fig. 6. Validation of Numerical Results with Experiments of Collector Thermal Efficiency.

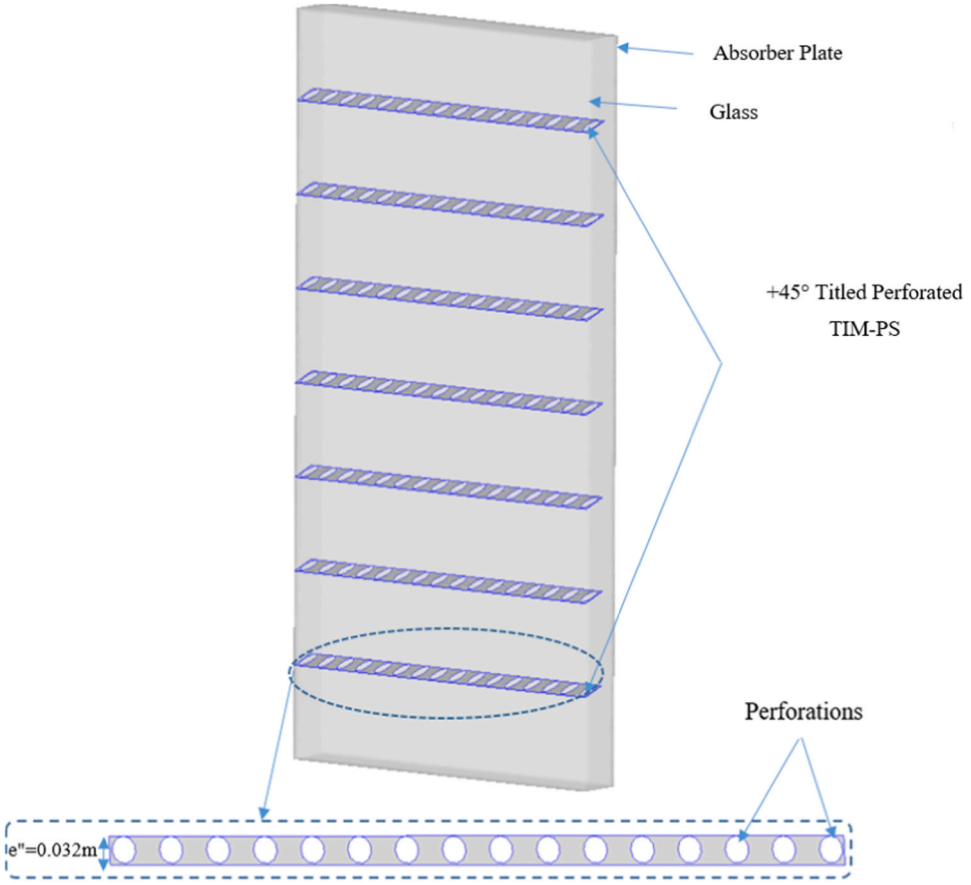

Fig. 7. Configuration of + 45° Inclined Perforated TIM-PS Sandwiched Between Absorber and Glass Cover in a Vertical Collector.

and December with six hours per day. Total sunshine during this period is around 221.63.

The ambient outdoor temperature and the solar radiation are provided for hourly climatic conditions in Monastir from 6 am to 6 pm. The climatic conditions belong to a place with Mediterranean weather all year round. The above mentioned data represent days with temperatures characteristic of winter, spring, summer and autumn in Monastir City.

Fig. 9 displays the diurnal fluctuations of the instantaneous solar radiation intensity and the ambient temperature on four specific days of solstices and equinoxesin Monastir City. The plots identify that the trend

Table 2
Materials Properties.

Items	Density (kg/m^3)	Specific Heat (J/kg K)	Thermal Conductivity (W/m K)	Absorptivity (—)	Emissivity (—)	Transmissivity (—)
Insulation	1040	1450	0.038	0.8	0.93	–
TIM-PS	2500	720	1	0.06	0.93	0.92
Absorber	2719	871	202.4	0.95	0.1	–
Air	1.225	1006.43	0.0242	–	–	–
Transparent cover	2500	720	1.4	0.06	0.93	0.84

Table 3
Geometrical Characteristics of the TIM-PS.

Parameters		Value
Width	**(m)**	0.935
Thickness	**(mm)**	1
Relative Height (e“/e)		0.8
Material		Polymethyl methacrylate (PMMA)

Table 4
Solar Radiation Conditions for MonastirIn Tunisia.

City	Monastir
Latitude	35°46 North
Longitude	10°49 East
Spectral Fraction	0.5
Sunshine Factor	0.55

of solar intensity (I) and temperatures are similar for different days. It was recognized that the temperatures and solar intensity are the most prominent in June (Summer Solstice), with an increase of solar intensity I up to 12–1 pm, and then ambient temperature increases with time. Ambient temperature was dependent on solar radiation, increasing in the morning to peak at noon and gradually decreasing in the afternoon. The weather data of the radiation and the temperature of the Monastir site have been taken by means of the web application 'PVGIS'.

The thermal efficiencies are a function of the inlet $T_{fi}$and outlet T_{fo}temperatures of the fluid and are determined using Eq.(3). The simulated thermal efficiency values for the conventional collector as well as for the novel collector are determined and visualized in Fig. 10.

The variations of the thermal efficiency of the FPC during the day as a function of solar radiation have been shown. The thermal efficiency expressed in Eq. (3) for both types of collectors varies only with ΔT.

Fig. 10 shows that the collectors' thermal efficiency is dramatically altered by the amount of solar radiation intensity for both collector configurations, for the range of environmental conditions.

The collector operating in natural convection mode is very sensitive to the inclination angle to the horizontal. The air flow inside the natural convection mode collector is significantly impacted by the inclination angle (Ammar et al., 2022). In this investigation case the treated collector is placed in a vertical position to facilitate the operating mode of the collector, by accelerating the air flow passage through the air duct. As the collector's vertical position is the most suitable for the air flow circulation by natural convection.

As it is shown in Fig. 10; the greatest thermal's improvement is noted in June (Summer Solstice).

Inside the air gap between the absorber plate and the transparent cover, a natural convection phenomenon known as the Rayleigh-Bénard instability taken place. This thermal instability leads to convective losses through the front of the collector. The introduction of tilted perforated TIM-PS reduces the thermal exchange between absorber and glass cover; consequently, increase the thermal performance of the collector.

The improvement in thermal performance is noticed for all the typical days, but the dependent of the improvement percentage to the day environmental conditions cannot be denied. Thus, the solar radiation intensity and the ambient temperature are essential factors in increasing the thermal heat losses. As with increasing the solar intensity and ambient temperature various collector's components heats up, then thermal exchange will be higher, consequently thermal efficiency is more affected and reduced when solar intensity is more important. For this reason, we can explain that the improvement in thermal

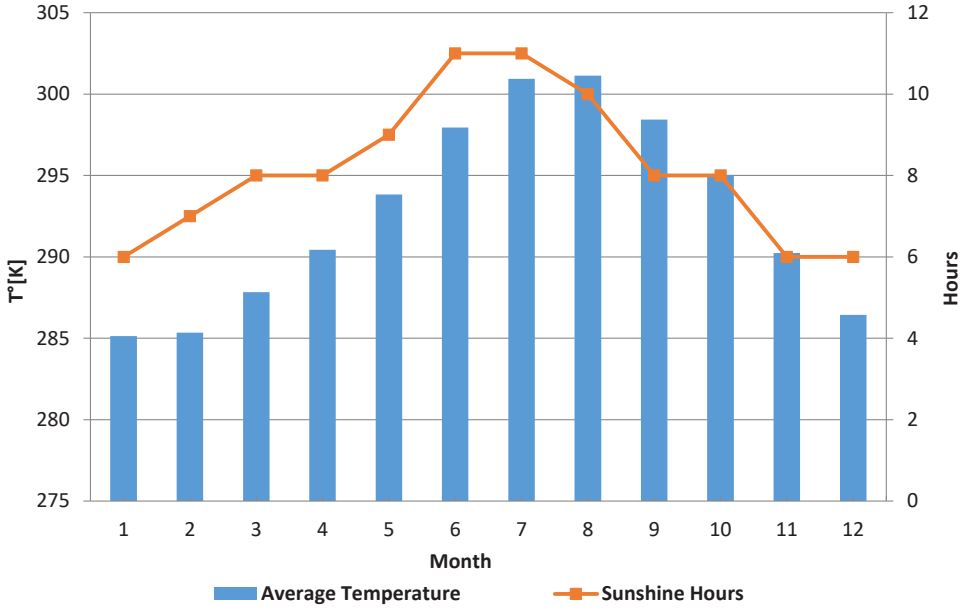

Fig. 8. Monthly Average Temperature and Sunshine Hours in Monastir City.

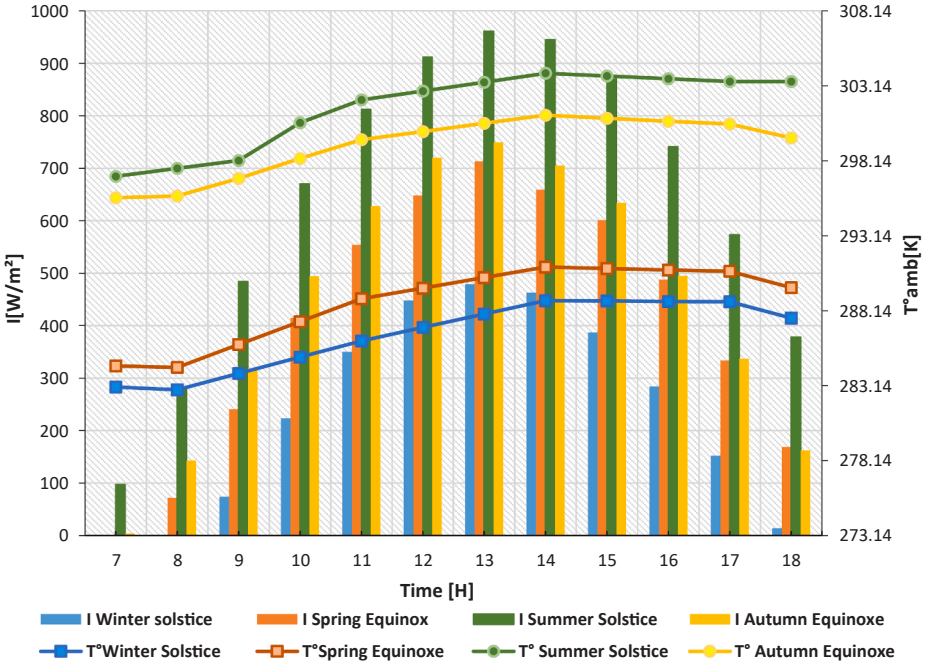

Fig. 9. Daily Fluctuations of the Instantaneous Solar Radiation Intensity and the Ambient Temperature on Four Specific Days of Solstices and Equinoxes in Monastir City.

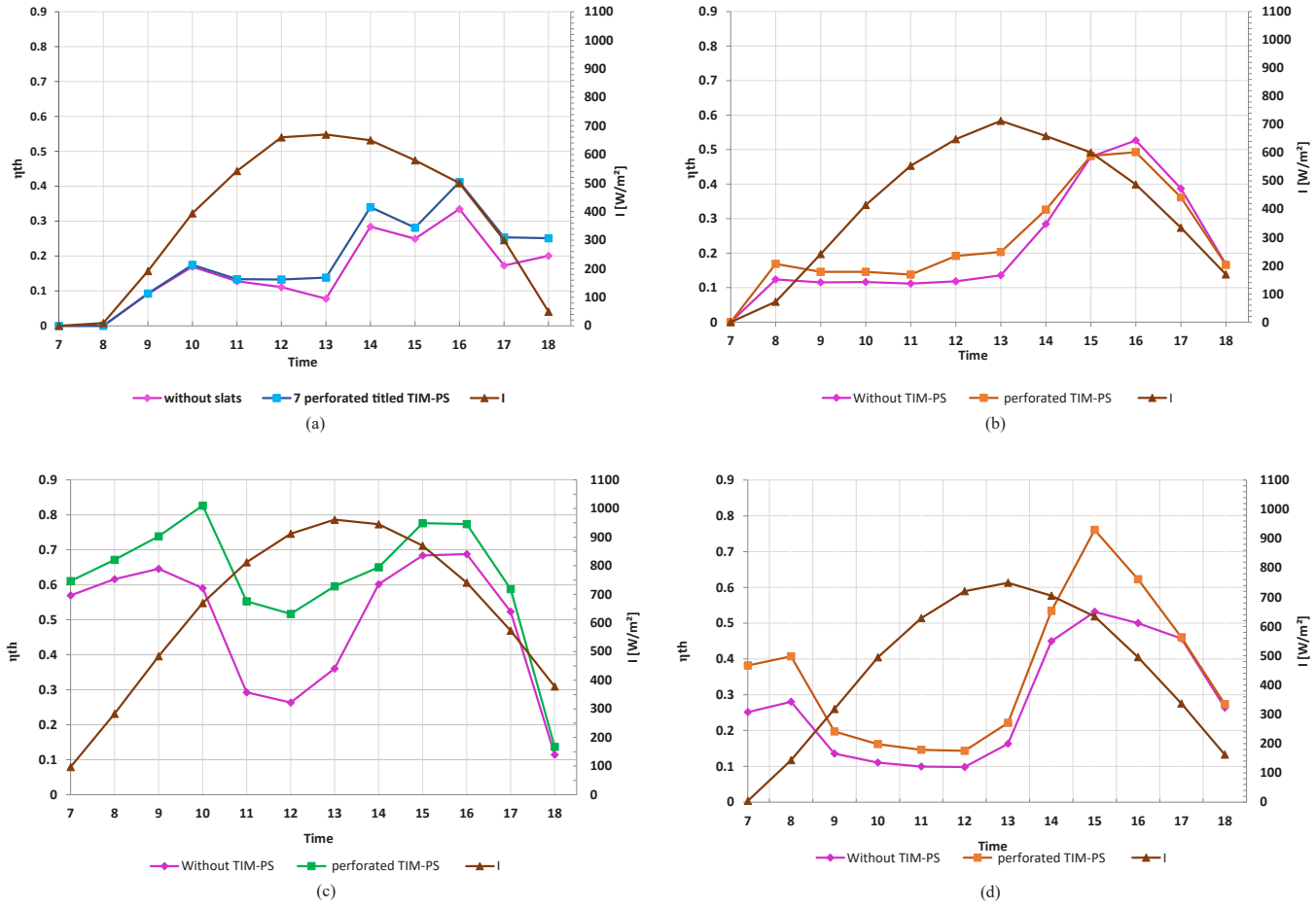

Fig. 10. Daily Variation of the Instantaneous Thermal Efficiency for A Collector with Perforated and Inclined TIM-PS in Comparison with A Conventional Collector in (a) December, (b) March, (c) June, (d) September.

performance will be different with time of the day as well as with the typical day for each season. It is noted clearly that the advantage of including tilted perforated TIM-PS is well validated in September. The convective losses which increase very significantly in the noon for a day in June Fig. 10.c will be reduced and blocked thanks to the presence of the tilted perforated TIM-PS. This improvement in thermal performance is very important in the noon, but even in the first hours of sunshine when the collector's components have not yet been sufficiently heated, the TIM-PS ensure some improvement in thermal performance.

Efficiency improvements thanks to the TIM-PS is noted for all seasons (Fig. 10.a, b, d). It is noted that the introduction of tilted perforated TIM-PS for use in winter day in December (Fig. 10.a) ensure a small thermal performance improvement, not well as for the summer days, but even acceptable.

In all investigated days the TIM-PS provide a good resistance to the onset of free convection losses, which consequently ameliorate the thermal performance during all the hours of the day.

For case in point, PMMA has greater than 90% transmittance at a wavelength of 600 nm. When incorporated into a flat plate solar collector façade, plastic slats break the air cavity among the glass cover and the absorber into a series of small air chambers, potentially raising the thermal insulation of the collector's façade system and preventing heat loss from the collector absorber to the outside environment. TIM attempts to convey resistance to heat flow without impeding sunlight transmission unlike an opaque insulation material.

There are days where the rate of amelioration in efficiency is very significant and others where it is less important. But even in these days, the advantage of including perforated tilted TIM-PS is validated all over the year. Which make the novel collector with TIM-PS is a great solution for improving the uses of a natural convection operating mode collector adapted to a changing environment climate.

The greatest improvement is noted in June (Summer Solstice); and given that in June the collector, due to the increase in radiation and ambient temperature, is a subject of very significant convective losses. This explains the low performance of the collector especially in the middle hours of the day after a few hours of sunrise when the collector has received sufficient radiation and its temperature has increased in a noticeable way.

When we see that the greatest increase in efficiency is noted during June, this clearly proves the major contribution provided by the transparent insulation material perforated and tilted slats in drastically reducing, or almost eliminating of convective losses through the glass.

It is generally recognized that in warm weather, the heating of air for the purpose of conditioning the atmosphere is not necessary, however, this heated air could be extremely beneficial for drying of agricultural products. This innovative collector, fitted with slats, could be perfectly suited for agricultural drying during the summer months, as it would accelerate the drying process and reduce the drying time considerably.

3.2.2. *Volume flow rate*

The variation of the natural convection airflow within the air duct below the absorber has been measured and can be seen in Fig. 11. The variation of the airflow is presented under a range of solar radiation intensity for a whole day. As can be clearly seen, the natural convection airflow depends significantly on the season and time of the same day, i.e. the airflow is strongly dependent on the solar radiation intensity.

Fig. 11.a illustrates the daily variation of air volume flow rate during a winter day in December. The improvement of the airflow in winter is noted, although it is not very significant, as in other cases for June and September. Fig. 11.c, d.

The TIM-PS accelerate the air flow, consequently they ameliorate significantly the collector's performance. As the value of I increases, in terms of volumetric flow, the discrepancy between conventional and newly created collectors appears increasingly significant. The highest circulation speed is obtained at 13 o′clock from a collector fitted with a TIM-PS device. Depending on its impact on the absorption plate, the

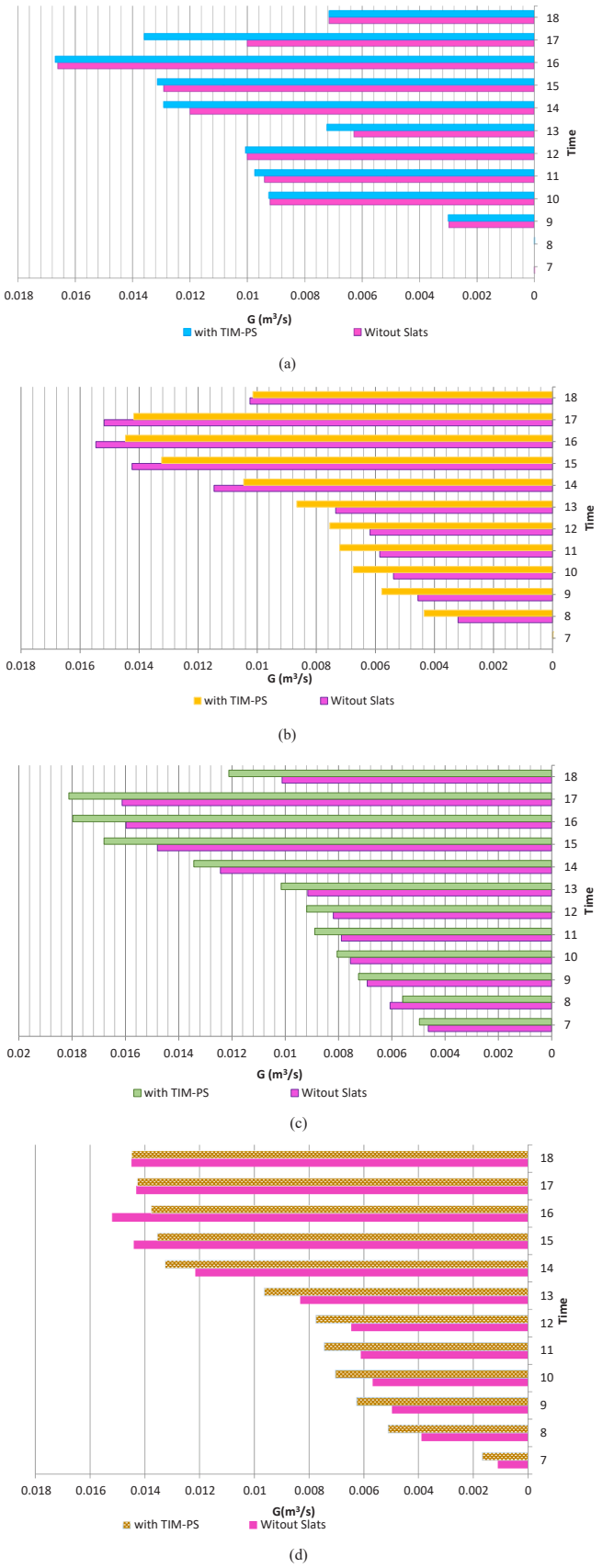

Fig. 11. Daily Variation of Volume Flow Rate for conventional and novel façade collectors in (a) December (b) March (c) June (d) September.

airflow varies according to the intensity of the solar radiation.

The air volume flow in the air duct under the absorber of the conventional collector as well as in the collector with innovative façade reaches its maximum values in summer (June), and its minimum in winter (December). This can be seen as the effect of the modulation of the rate of thermal radiation: in summer, the very high level of this radiation reaches the surface of the absorber, resulting in a high flow velocity of the air in the lower part of the plate, compared with the lower flow velocity in winter.

Furthermore, it is the effects of shading, of the sun's rays hitting the absorber plate and of the presence of the slats that cause the air flow in the duct under the absorber plate to vary. Notwithstanding the fact that the slats create an unenlightened zone, the transmission capacity of PMMA makes it possible to correct this unenlightened zone and reduce it to nothing thanks to the addition of these slats.

Fig. 12 presents the streamlines for an air gap fitted with perforated slats tilted at + 45°. Inside the air gap collector, the structure of natural convection flow is shown as regular "rolls of Bénard", whose rupture is ensured in particular by the TIM-PS system.

The single-cell structure of the airflow is split into a multitude of microcells with curved contours because the TIM-PS is inclined.

First of all, it is important to point out that the distribution of the airflow differs greatly depending on the degree to which the TIM-PS slopes. After being heated by the absorber due to the reduction in density, it automatically rises to the top, touches the "cold" of the transparent panel and cools down, only to fall back down again. The direction of rotation is then imposed as part of the determination of that of the warm absorber surface at the bottom against that of the cooling plate at the top. The air current rotates in a clockwise direction, linked to these two elements, and is reflected on the area close to the absorber's hot plate as TIM-PS tilts downwards. The rest of the air flows back towards the base of the system. Almost all of this flow passes through areas close to the hot face and the corners of the TIM-PS system's inclined module. There is also significant condensation near the warm layer of air. The sloping design of the slats at an angle of + 45° hampers the shaping of homogeneous rolls as much as it breaks the continuity of homogeneous rolls. The angle of inclination over 45° restricts the freedom of motion, thereby limiting the ability of the rollers to be constructed. The slats should not be filled, to prevent shading and ensure that the light beam is directed as strongly as possible towards the surface of the absorber. TIM-PS sloped slats, for their part, are capable of slowing down the movement of heat due to natural convection in the air gap, while enabling light to penetrate the absorber plate. To be more accurate, a high rate of light radiation from the sun is allowed to pass through the transparent perforated slats and reach the absorption base. However, care must be taken to ensure that the thermal energy is not lost through convection of the surrounding air trapped in the air space.

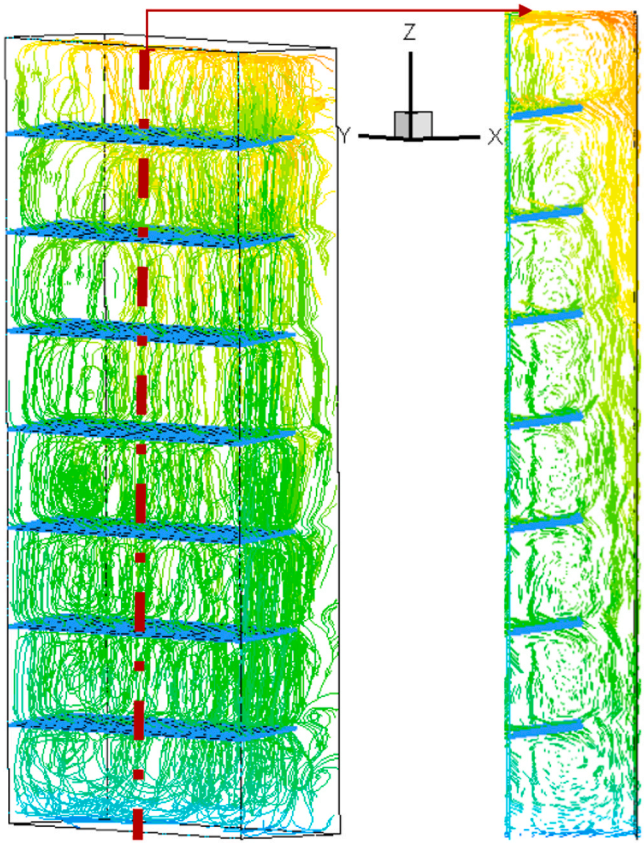

Fig. 12. Streamlines Inside the Air Gap Containing Perforated Tilted TIM-PS Inclined with A Slice On Planes (xoz).

Because of their performance, the sloped and perforated TIM-PS have a multiplying action that divides the air space into different small cells. The slats themselves provide enhanced protection against free convection and interference with thermal radiation transferred from the glass to the absorber. It is strategically advisable to use transparent insulating materials (TIM) sandwiched between the glass and the absorber of a flat-plate solar collector to increase the thermal performance of the device and preserve access to the sun's light and heat.

Transparent insulation materials parallel slats have made a substantial contribution to the reduction of the convective heat losses. They have dynamically regulated solar energy, saving energy and improving collector performance. Transparent insulation material parallel slats (TIM-PS) integrated into the collector façade can increase the thermal resistance of the collector, thereby reducing heat loss. In this study, these advanced technologies are used to form a new TIM-PS collector façade plate system for adaptive performance control and thermal insulation improvement.

3.2.3. *Economic and weight analyses*

Before implementing the innovative design of the flat plate collector and once it has proved how well it performs, two major indicators of potential impact require careful study in depth analysis of the contribution of the slats to the optimization of the air collector. This study should focus firstly on the economical aspect: the economic feasibility or economic study, and secondly on the issue involved in the final weight of the collector.

The initial cost of the reference collector, which is assumed to range at $350 per m^2, will remain unchanged, but we will actually examine the price of the changes brought about by the introduction of the slats.

The main component used in the slats is poly-methyl-methacrylate (PMMA). The cost of TIM-PS made with PMMA, shown in Table 5, is therefore included in the cost analysis. The unit cost of the slat is determined to be of the order of $3.55. This means that the set of slats required to ensure improved high performance will not exceed $25. The cost of the slats is therefore marginal in relation to the collector 's cost.

As weight is a reliable parameter, it is very relevant to calculate the extra weight that will be added to the collector when the slats are added.

The solar collector was manufactured with a weight of approximately 45 kg. The new approach in this study introduces perforated TIM-PS techniques. Considerable applicability and reduced weight are considered promising advantages of using perforated slats.

As shown in Table 5, the weight of the slat is 22.115 g, so only

Table 5
Cost and weight of TIM-PS.

Components	Quantity	weight per unit [g]	Cost per unit $	Total weight [g]	Total cost $
Perforated TIM-PS	7	22.115	3.55	154.81	24.8

154.81 g needs to be added to the initial weight of the collector by the set of slats considered.

The weight added by the insertion of the slats is insignificant compared to the initial weight of the collector.

The improvements in thermal performance obtained with the slat-type collector are realized without an excessive investment. In fact, the innovative collector is the result of the addition of seven slats weighing a total of 155 g, at an extra cost of $25.

4. Conclusion

The aim of this article is to assess the effectiveness of inserting the TIM-PS into the collector, then to evaluate the estimated cost of the slats and finally to evaluate the final weight of the collector.

Based on the hourly numerical results of the new façade collector for different climates of Monastir we can conclude that:

- In terms of determining the thermal efficiency of the collector with the new façade for Monastir; the performance of the FPC with the TIM-PS is strongly related to climatic conditions. For any given constant value of heat flux, the performance of the FPC operating with natural convection is the highest for the new façade collector. For high solar radiation intensity, it could achieve higher conversion efficiency than a conventional collector. The innovative FPC façade comprising seven perforated+ 45°tilted TIM-PS offered the potential to improve the thermal efficiency reaching 83% in June, 76% in September, 53% in March and 42% in December. The novel design of a natural convection mode collector is adapted to a changing Mediterranean climate.
- In terms of determining the volume flow rate, the TIM-PS accelerate the air velocity through the air duct, thus they enhance the air circulation by natural convection process.
- On behalf of the economic coast; the innovative design of the collector operating in natural convection mode provides a higher efficiency compared to existing collectors, allowing the collector to be trusted for annual service. The new retrofit technique is quite simple and inexpensive and at the same time offers a very significant net improvement.
- The new collector's design is marked by very high thermal insulation capacity, high cost effectiveness and reliability. The new solar collector is made with seven additional slats, weighing a total of 155 g, at an additional cost of $25. It has the advantages of being lightweight, the TIM-PS have the capacity to be easily dismantled and replaced compared to rigid slats, which finally extends their wide range of practical applications.

The success of the indirect air heating system in natural convection mode with TIM-PS in a Mediterranean climate is proven by the results obtained in this work.

For future work, the proposal will be to build experimentally this design of solar air heating collector operating both in winter for air conditioning and in summer for agricultural drying, capable of operating during hours without sunlight, using an energy storage process.

Author statement

All authors have seen and approved the final version of the manuscript being submitted. They warrant that the article is the authors' original work, hasn't received prior publication and isn't under consideration for publication elsewhere.

Declaration of Competing Interest

The authors declare that they have no known competing financial interests or personal relationships that could have appeared to influence the work reported in this paper.

Data Availability

No data was used for the research described in the article.

References

Altaç, Z., Uğurlubilek, N., 2016. Assessment of turbulence models in natural convection from two- and three-dimensional rectangular enclosures. Int. J. Therm. Sci. 107, 237–246.

Ammar, M., Mokni, A., Mhiri, H., Bournot, P., n.d. Performance optimization of flat plate solar collector through the integration of different slats arrangements made of transparent insulation material. Sustainable Energy Technologies and Assessments 46,101237.

Ammar, M., Mokni, A., Mhiri, H., Bournot, P., 2022. Parametric investigation on the performance of natural convection flat plate solar air collector with additional transparent insulation material parallel slats (TIM-PS). Sol. Energy 231, 379–401.

Bahria, S., Amirat, M., Boumediene, T.H., 32, B.P., Alia, E., Ezzouar, B., Alger, A., 2013. Influence de l'adjonction des chicanes longitudinales sur les performances d'un capteur solaire plan à air. Rev. Des. Energ. Renouvelables 16, 51–63.

Choi, S.K., Kim, S.O., 2012. Turbulence modeling of natural convection in enclosures: a review. J. Mech. Sci. Technol. 26, 283–297.

Duffie, J.A., Beckman, W.A., McGowan, J., 1985. Solar engineering of thermal processes. Am. J. Phys. 53 (Issue 4).

Eismann, R., 2015. Accurate analytical modeling of flat plate solar collectors: extended correlation for convective heat loss across the air gap between absorber and cover plate. Sol. Energy 122, 1214–1224.

Fuji, M., Takai, C., Watanabe, H., Fujimoto, K., 2015. Improved transparent thermal insulation using nano-spaces. Adv. Powder Technol. 26, 857–860.

Garcia, R.P., Oliveira, S. del R., Scalon, V.L., 2019. Thermal efficiency experimental evaluation of solar flat plate collectors when introducing convective barriers. Sol. Energy 182, 278–285.

Gorgolis, G., Karamanis, D., 2016. Solar energy materials for glazing technologies. Sol. Energy Mater. Sol. Cells 144, 559–578.

Groenhout, N.K., Behnia, M., Morrison, G.L., 2002. Experimental measurement of heat loss in an advanced solar collector. Exp. Therm. Fluid Sci. 26, 131–137.

Hollands, K.G.T., 1965. Honeycomb devices in flat-plate solar collectors. Sol. Energy 9, 159–164.

Hollands, K.G.T., Iynkaran, K., Ford, C., Platzer, W.J., 1992. Manufacture, solar transmission, and heat transfer characteristics of large-celled honeycomb transparent insulation. Sol. Energy 49, 381–385.

Jia, H., Zhu, J., Debeli, D.K., Li, Z., Guo, J., 2018. Solar thermal energy harvesting properties of spacer fabric composite used for transparent insulation materials. Sol. Energy Mater. Sol. Cells 174, 140–145.

Kim, S., Jeong, H., Park, J.Y., Baek, S.Y., Lee, A., Choi, S.H., 2019. Innovative flat-plate solar collector (FPC) with coloured water flowing through a transparent tube. RSC Adv. 9, 24192–24202.

Ming, Y., Sun, Y., Liu, Xin, Liu, Xiao, Wu, Y., 2022. Optical evaluation of a smart transparent insulation material for window application. Energy Convers. Management:X16, 100315.

Paneri, A., Wong, I.L., Burek, S., 2019. Transparent insulation materials: an overview on past, present and future developments. Sol. Energy 184, 59–83.

Plaizer, W.J., 1992. Data for plastic honeycomb-type structures, 49, 359–369.

Rani, P., Tripathy, P.P., 2020. Thermal characteristics of a flat plate solar collector: influence of air mass flow rate and correlation analysis among process parameters. Sol. Energy 211, 464–477.

Rosenfeld, J.L.J., Platzer, W.J., van Dijk, H., Maccari, A., 2001. Modelling the optical and thermal properties of complex glazing: overview of recent developments. Sol. Energy 69, 1–13.

Saini, V., Tiwari, S., Tiwari, G.N., 2017. Environ economic analysis of various types of photovoltaic technologies integrated with greenhouse solar drying system. J. Clean. Prod. 156, 30–40.

Schaefer, R., Lowrey, P., 1992. The optimum design of honeycomb solar ponds and a comparison with salt gradient ponds. Sol. Energy 48, 69–78.

Sun, Y., Wu, Y., Wilson, R., 2017. Analysis of the daylight performance of a glazing system with Parallel Slat Transparent Insulation Material (PS-TIM). Energy Build. 139, 616–633.

Sun, Y., Liu, Xin, Ming, Y., Liu, Xiao, Mahon, D., Wilson, R., Liu, H., Eames, P., Wu, Y., 2021. Energy and daylight performance of a smart window: window integrated with thermotropic parallel slat-transparent insulation material. Appl. Energy 293, 116826.

Tuncer, A.D., Khanlari, A., Sözen, A., Gürbüz, E.Y., Şirin, C., Gungor, A., 2020. Energy-exergy and enviro-economic survey of solar air heaters with various air channel modifications. Renew. Energy 160, 67–85.

Varol, Y., Oztop, H.F., 2008. A comparative numerical study on natural convection in inclined wavy and flat-plate solar collectors. Build. Environ. 43, 1535–1544.